# Measurement of Branching Fractions for $B \to \eta_c K^{(*)}$ Decays

F. Fang[7], T. Hojo[30], K. Abe[8], K. Abe[40], T. Abe[41], I. Adachi[8], H. Aihara[42], M. Akatsu[22], Y. Asano[47], T. Aso[46], V. Aulchenko[1], A. M. Bakich[38], Y. Ban[34], E. Banas[26], A. Bay[18], P. K. Behera[48], I. Bizjak[13], A. Bondar[1], A. Bozek[26], M. Bračko[20,13], J. Brodzicka[26], T. E. Browder[7], B. C. K. Casey[7], P. Chang[25], Y. Chao[25], K.-F. Chen[25], B. G. Cheon[37], R. Chistov[12], S.-K. Choi[6], Y. Choi[37], Y. K. Choi[37], M. Danilov[12], A. Drutskoy[12], S. Eidelman[1], V. Eiges[12], Y. Enari[22], C. Fukunaga[44], N. Gabyshev[8], A. Garmash[1,8], T. Gershon[8], B. Golob[19,13], T. Hara[30], N. C. Hastings[21], H. Hayashii[23], M. Hazumi[8], E. M. Heenan[21], T. Higuchi[42], L. Hinz[18], T. Hokuue[22], Y. Hoshi[40], W.-S. Hou[25], H.-C. Huang[25], T. Igaki[22], Y. Igarashi[8], T. Iijima[22], K. Inami[22], A. Ishikawa[22], R. Itoh[8], H. Iwasaki[8], Y. Iwasaki[8], H. K. Jang[36], J. H. Kang[51], J. S. Kang[15], P. Kapusta[26], N. Katayama[8], H. Kawai[2], Y. Kawakami[22], T. Kawasaki[28], H. Kichimi[8], D. W. Kim[37], Heejong Kim[51], H. J. Kim[51], H. O. Kim[37], Hyunwoo Kim[15], S. K. Kim[36], K. Kinoshita[4], S. Kobayashi[34], S. Korpar[20,13], P. Križan[19,13], P. Krokovny[1], R. Kulasiri[4], Y.-J. Kwon[51], J. S. Lange[5,33], G. Leder[11], S. H. Lee[36], J. Li[35], D. Liventsev[12], R.-S. Lu[25], J. MacNaughton[11], F. Mandl[11], S. Matsumoto[3], T. Matsumoto[44], W. Mitaroff[11], K. Miyabayashi[23], H. Miyake[30], H. Miyata[28], G. R. Moloney[21], T. Mori[3], T. Nagamine[41], Y. Nagasaka[9], T. Nakadaira[42], E. Nakano[29], M. Nakao[8], H. Nakazawa[3], J. W. Nam[37], Z. Natkaniec[26], S. Nishida[16], O. Nitoh[45], S. Noguchi[23], T. Nozaki[8], S. Ogawa[39], T. Ohshima[22], T. Okabe[22], S. Okuno[14], S. L. Olsen[7], Y. Onuki[28], H. Ozaki[8], P. Pakhlov[12], C. W. Park[15], H. Park[17], K. S. Park[37], J.-P. Perroud[18], M. Peters[7], L. E. Piilonen[49], F. J. Ronga[18], N. Root[1], M. Rozanska[26], K. Rybicki[26], H. Sagawa[8], S. Saitoh[8], Y. Sakai[8], H. Sakamoto[16], M. Satapathy[48], O. Schneider[18], S. Schrenk[4], C. Schwanda[8,11], S. Semenov[12], K. Senyo[22], R. Seuster[7], M. E. Sevior[21], H. Shibuya[39], B. Shwartz[1], V. Sidorov[1], N. Soni[31], S. Stanič[47,⋆], M. Starič[13], A. Sugi[22], A. Sugiyama[22], K. Sumisawa[8], T. Sumiyoshi[44], K. Suzuki[8], S. Suzuki[50], T. Takahashi[29], F. Takasaki[8], N. Tamura[28], J. Tanaka[42], M. Tanaka[8], G. N. Taylor[21], Y. Teramoto[29], S. Tokuda[22], T. Tomura[42], K. Trabelsi[7], T. Tsuboyama[8], T. Tsukamoto[8], S. Uehara[8], K. Ueno[25], S. Uno[8], Y. Ushiroda[8], S. E. Vahsen[32], G. Varner[7], K. E. Varvell[38], C. C. Wang[25], C. H. Wang[24], J. G. Wang[49], M.-Z. Wang[25], Y. Watanabe[43], E. Won[15], B. D. Yabsley[49], Y. Yamada[8], A. Yamaguchi[41], Y. Yamashita[27], M. Yamauchi[8], H. Yanai[28], J. Yashima[8], M. Yokoyama[42], Y. Yuan[10], Y. Yusa[41], C. C. Zhang[10], J. Zhang[47], Z. P. Zhang[35], V. Zhilich[1], and D. Žontar[47]

[1]Budker Institute of Nuclear Physics, Novosibirsk
[2]Chiba University, Chiba
[3]Chuo University, Tokyo
[4]University of Cincinnati, Cincinnati OH
[5]University of Frankfurt, Frankfurt
[6]Gyeongsang National University, Chinju
[7]University of Hawaii, Honolulu HI
[8]High Energy Accelerator Research Organization (KEK), Tsukuba
[9]Hiroshima Institute of Technology, Hiroshima
[10]Institute of High Energy Physics, Chinese Academy of Sciences, Beijing
[11]Institute of High Energy Physics, Vienna
[12]Institute for Theoretical and Experimental Physics, Moscow
[13]J. Stefan Institute, Ljubljana
[14]Kanagawa University, Yokohama
[15]Korea University, Seoul
[16]Kyoto University, Kyoto
[17]Kyungpook National University, Taegu
[18]Institut de Physique des Hautes Énergies, Université de Lausanne, Lausanne
[19]University of Ljubljana, Ljubljana
[20]University of Maribor, Maribor
[21]University of Melbourne, Victoria
[22]Nagoya University, Nagoya
[23]Nara Women's University, Nara
[24]National Lien-Ho Institute of Technology, Miao Li
[25]National Taiwan University, Taipei
[26]H. Niewodniczanski Institute of Nuclear Physics, Krakow
[27]Nihon Dental College, Niigata
[28]Niigata University, Niigata
[29]Osaka City University, Osaka
[30]Osaka University, Osaka
[31]Panjab University, Chandigarh
[32]Princeton University, Princeton NJ

1

$^{33}$RIKEN BNL Research Center, Brookhaven NY
$^{34}$Saga University, Saga
$^{35}$University of Science and Technology of China, Hefei
$^{36}$Seoul National University, Seoul
$^{37}$Sungkyunkwan University, Suwon
$^{38}$University of Sydney, Sydney NSW
$^{39}$Toho University, Funabashi
$^{40}$Tohoku Gakuin University, Tagajo
$^{41}$Tohoku University, Sendai
$^{42}$University of Tokyo, Tokyo
$^{43}$Tokyo Institute of Technology, Tokyo
$^{44}$Tokyo Metropolitan University, Tokyo
$^{45}$Tokyo University of Agriculture and Technology, Tokyo
$^{46}$Toyama National College of Maritime Technology, Toyama
$^{47}$University of Tsukuba, Tsukuba
$^{48}$Utkal University, Bhubaneswer
$^{49}$Virginia Polytechnic Institute and State University, Blacksburg VA
$^{50}$Yokkaichi University, Yokkaichi
$^{51}$Yonsei University, Seoul
$^{\star}$on leave from Nova Gorica Polytechnic, Slovenia

We report measurements of branching fractions for charged and neutral $B \to \eta_c K$ decays where the $\eta_c$ meson is reconstructed in the $K_S^0 K^\pm \pi^\mp, K^+ K^- \pi^0, K^{*0} K^- \pi^+$ and $p\bar{p}$ decay channels. The neutral $B^0$ channel is a $CP$ eigenstate and can be used to measure the $CP$ violation parameter $\sin 2\phi_1$. We also report the first observation of the $B^0 \to \eta_c K^{*0}$ mode. The results are based on an analysis of 29.1 fb$^{-1}$ of data collected by the Belle detector at KEKB.

PACS numbers: 13.20.He, 13.25.Hw, 13.60.Rj

The decay mode $B \to \eta_c K$ proceeds by a spectator $b \to c\bar{c}s$ transition with internal $W$-emission as in the $CP$ eigenstate $B^0 \to J/\psi K_S^0$. The neutral decay mode $B^0 \to \eta_c K_S^0$ has therefore been used to measure the $CP$ violation parameter $\sin 2\phi_1$ [1], [2], [3]. Measurements of branching fractions for $B \to \eta_c K^{(*)}$ decay modes are also useful in the study of the dynamics of hadronic $B$ decay [4]. However, in contrast to $B^0 \to J/\psi K_S^0$, the $\eta_c$ meson must be reconstructed from hadronic decays rather than from a leptonic final state with relatively low combinatorial background. In this paper, we report new measurements of $B \to \eta_c K$ branching fractions with the $\eta_c$ meson reconstructed in the $K_S^0 K^+\pi^-$, $K^- K^+\pi^0$, $K^{*0}K^-\pi^+$ and $p\bar{p}$ channels [5]. These signals are large enough to be used to determine the mass and width of the $\eta_c$ meson. We also report the first observation of the related decay mode $B^0 \to \eta_c K^{*0}$. When $K^{*0} \to K_S^0 \pi^0$, this decay mode is also a $CP$ eigenstate.

We use a 29.1 fb$^{-1}$ data sample, which contains 31.3 million produced $B\bar{B}$ pairs, collected with the Belle detector at the KEKB asymmetric-energy $e^+e^-$ (3.5 on 8 GeV) collider [6]. KEKB operates at the $\Upsilon(4S)$ resonance ($\sqrt{s} = 10.58$ GeV) with a peak luminosity that now exceeds $7 \times 10^{33}$ cm$^{-2}$s$^{-1}$. The Belle detector is a large-solid-angle magnetic spectrometer that consists of a three-layer silicon vertex detector (SVD), a 50-layer central drift chamber (CDC), a mosaic of aerogel threshold Čerenkov counters (ACC), time-of-flight scintillation counters (TOF), and an array of CsI(Tl) crystals (ECL) located inside a superconducting solenoid coil that provides a 1.5 T magnetic field. An iron flux-return located outside of the coil is instrumented to identify $K_L$ and muons (KLM). The detector is described in detail elsewhere [7].

We select well measured charged tracks with impact parameters with respect to the interaction point of less than 0.5 cm in the radial direction and less than 3 cm in the beam direction ($z$). These tracks are required to have $p_T > 50$ MeV/$c$.

Particle identification likelihoods for the pion and kaon particle hypotheses are calculated by combining information from the TOF and ACC systems with $dE/dx$ measurements in the CDC. To identify kaons (pions), we apply a mode-dependent requirement on the kaon (pion) likelihood ratio, $L_K/(L_\pi + L_K)$ ($L_\pi/(L_\pi + L_K)$). The requirement $L_K/(L_\pi + L_K) > 0.5$ is used for the $\eta_c \to K_S^0 K^-\pi^+$ mode. For other modes, we require $L_K/(L_\pi + L_K) > 0.6$, which is 88% efficient for kaons with a 8.5% misidentification rate for pions. For the $\eta_c \to K^+K^-\pi^0$ mode, the kaon likelihood ratio is required to be greater than 0.8 for those charged kaons that come directly from the $B$ rather than from the $\eta_c$ candidate. In addition, we remove all kaon candidates that are consistent with being either protons or electrons.

Protons and antiprotons are identified using all particle ID systems and are required to have proton likelihood ratios ($L_p/(L_p + L_K)$ and $L_p/(L_p + L_\pi)$) greater than 0.4. Proton candidates that are electron-like according to the information recorded by the CsI(Tl) calorimeter are vetoed. This selection is 95% efficient for protons with a 12% kaon misidentification rate.

We select $K_S$ candidates from $\pi^+\pi^-$ candidates that lie within the mass window 0.482 GeV/$c^2 < M(\pi^+\pi^-) <$ 0.514 GeV/$c^2$ ($\pm 4\sigma$). The flight length of the $K_S$ is required to be greater than 0.2 cm. The difference in the angle, in the $x-y$ plane, between a vector from the beam spot to the $K_S$ vertex and the $K_S$ flight direction is required to satisfy $\Delta\phi < 0.1$ rad.

$K^{*0}$ candidates are reconstructed in the $K^+\pi^-$ mode. For $\eta_c \to K^{*0}K^-\pi^+$, we require the $K^+\pi^-$ invariant mass to be between 0.817 and 0.967 GeV/$c^2$. For the $B^0 \to \eta_c K^{*0}$ mode, the $K^{*0}$ mass must lie in the range between 0.801 and 0.991 GeV/$c^2$.

Neutral pion candidates are selected from pairs of ECL clusters with invariant mass within $\pm 16$ MeV of the nominal $\pi^0$ mass and momenta above 350 MeV/c. The photons must have energy above 50 MeV if they lie in the barrel region of the calorimeter and above 200 MeV if they are detected in the endcap.

To reconstruct signal candidates in the $B^+ \to \eta_c K^+$ and $B^0 \to \eta_c K^0$ modes, we form combinations of charged or neutral kaons and $\eta_c$ candidates. The $\eta_c$ is reconstructed in the $K_S^0 K^+\pi^-$, $K^- K^+\pi^0$, $K^{*0}K^-\pi^+$ and $p\bar{p}$ decay modes. The $\eta_c$ candidate is required to have invariant mass in the range $2.920 < M_{\eta_c} < 3.035$ GeV/$c^2$ for the $K^- K^+\pi^0$ mode and $2.935 < M_{\eta_c} < 3.035$ GeV/$c^2$ for all other modes. The charged daughters of the $\eta_c$ are required to satisfy a vertex constrained fit with a mode-dependent $\chi^2$ requirement [8].

To isolate the signal, we form the beam-energy constrained mass, $M_{\mathrm{bc}} = \sqrt{E_{\mathrm{beam}}^2 - \vec{P}_{\mathrm{recon}}^2}$, and energy difference $\Delta E = E_{\mathrm{recon}} - E_{\mathrm{beam}}$ in the $\Upsilon(4S)$ center of mass frame. Here $E_{\mathrm{beam}}$, $E_{\mathrm{recon}}$ and $\vec{P}_{\mathrm{recon}}$ are the beam energy, the reconstructed energy and the reconstructed momentum of the signal candidate, respectively. The signal region for $\Delta E$ in all modes except for $\eta_c \to K_S^0 K^-\pi^+$ is $\pm 2.5\sigma$, where $\sigma$ is the mode-dependent resolution and ranges from $\pm 25$ MeV for $\eta_c \to p\bar{p}$ to the range $-55, +45$ MeV for $\eta_c \to K^- K^+\pi^0$. In the low background $\eta_c \to K_S^0 K^-\pi^+$ mode, the region is extended to $\pm 35$ MeV, ($\pm 3.5\sigma$). The signal region for $M_{\mathrm{bc}}$ is 5.270 GeV/$c^2 < M_{\mathrm{bc}} < 5.290$ GeV/$c^2$. The resolution in beam-energy constrained mass is 2.8 MeV/$c^2$ and is dominated by the beam energy spread of KEKB.

Several event topology variables provide discrimination between the large continuum ($e^+e^- \to q\bar{q}$, where $q = u, d, s, c$) background, which tends to be collimated

along the original quark direction, and more spherical $B\bar{B}$ events. We first remove events with $R_2 > 0.5$, where $R_2$ is the normalized second Fox-Wolfram moment. We form a likelihood ratio using two variables. Six modified Fox-Wolfram moments and the cosine of the thrust angle are combined into a Fisher discriminant [9]. For signal MC and continuum data, we then form probability density functions for this Fisher discriminant, and the cosine of the $B$ decay angle with respect to the $z$ axis ($\cos\theta_B$). The signal (background) probability density functions are multiplied together to form a signal (background) likelihood $\mathcal{L}_S$ ($\mathcal{L}_{BG}$). A mode-dependent likelihood ratio requirement $\mathcal{L}_S/(\mathcal{L}_S + \mathcal{L}_{BG})$ is then imposed.

Using a sample of 57 million $B\bar{B}$ Monte Carlo events with a model of $b \to c$ decays, we investigate backgrounds from other $B$ decay modes. In the $\eta_c \to p\bar{p}$ mode, no such backgrounds are found. In other modes, some background is observed but it can be removed by application of mode-dependent vetos on invariant mass combinations that are consistent with the $D$, $D_s$, $\chi_{c1}$, $J/\psi$, $\psi(2S)$ or $\eta_c(2S)$ masses. For example, in the $B^+ \to \eta_c K^+$, $\eta_c \to K^+K^-\pi^0$ mode, we find there is background from the decay chain $B^+ \to \bar{D}^0\rho^+$, $\bar{D}^0 \to K^-K^+$, $\rho^+ \to \pi^+\pi^0$. This background is removed by requiring that the $K^-K^+$ invariant mass be inconsistent with the $D^0$ mass.

We fit the $M_{\rm bc}$ distribution to the sum of a signal Gaussian and a background function that behaves like phase space near the kinematic boundary [10]. The width of the Gaussian is fixed from MC simulation while the mean is determined from $B^+ \to \bar{D}^0\pi^+$ data. The shape parameter of the background function is determined from $\Delta E$ sideband data. The signal yield was determined by fits to the individual $M_{\rm bc}$ distributions for each mode. The yields and significances [11] for these fits are given in Table I. Significant signals are observed in all decay modes except for $B^0 \to \eta_c K^0$, $\eta_c \to K^{*0}K^-\pi^+$. For this mode, we calculate an upper limit based on the number of events observed in the $M_{\rm bc}$ signal region (4) and the expected number of background events (2) based on the fit. We use the Feldman-Cousins procedure [12], and reduce the efficiency by one sigma of the systematic error in the calculation [13]. The detection efficiencies for all modes were determined from a GEANT based Monte Carlo simulation.

For illustration, in Fig. 1, we show the beam-energy constrained mass and $\Delta E$ distributions for the signal candidates in all the decay modes except for $B^0 \to \eta_c K_S^0$, $\eta_c \to K^{*0}K^-\pi^+$. In the $M_{\rm bc}$ distribution, we observe a signal of $195 \pm 17$ events.

As a consistency check, we also determine the yield from a fit to the $\Delta E$ distribution with a double Gaussian for signal and a linear background function with slope determined from the $M_{\rm bc}$ sideband. The results of these fits are also given in Table I. The fit to the $\Delta E$ distri-
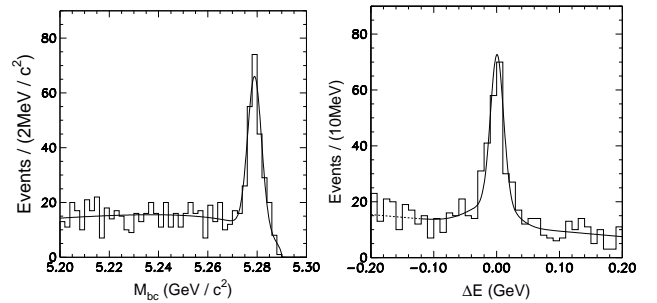


FIG. 1. (a) $M_{\rm bc}$ and (b) $\Delta E$ distributions for $B \to \eta_c K$ candidates in all the decay modes.

bution for all modes combined gives an integrated yield of $188 \pm 17$ events in the signal region. In the fits to the $\Delta E$ distribution, the region with $\Delta E < -120$ MeV is excluded to avoid contributions from modes with additional particles such as $B \to \eta_c K^*$.

After removing the requirements on $\eta_c$ invariant mass, we also verify that the signal yield for $\eta_c$ candidates in the $M_{\rm bc}$, $\Delta E$ signal region is consistent with the result used for the branching fraction determination. The $\eta_c$ invariant mass distribution for signal candidates is shown in Fig. 2. Fitting to a Breit-Wigner convolved with the resolution determined from MC, we find an intrinsic width $\Gamma(\eta_c) = 29 \pm 8 \pm 6$ MeV and a mass $M(\eta_c) = 2979.6 \pm 2.3 \pm 1.6$ MeV. The systematic errors in the width and mass measurements include the effects of varying the background shape, the small difference between data and MC detector resolutions, and possible binning effects. The results are consistent with world averages and comparable in precision to the best individual measurements [14]. The yield is $182 \pm 25$ events. We also observe a clear signal of $66 \pm 18$ events from $B \to J/\psi K$, where the $J/\psi$ is reconstructed in hadronic decay modes, that has a $J/\psi$ mass and yield that are consistent with values obtained for the $J/\psi \to \ell^+\ell^-$ decay mode.
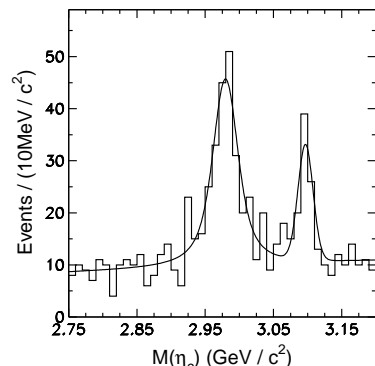


FIG. 2. Candidate $M(\eta_c)$ invariant mass distribution for events in the $M_{\rm bc}$ and $\Delta E$ signal region. Signals at the $\eta_c$ and $J/\psi$ masses from $B \to \eta_c K$ and $B \to J/\psi K$ decays are visible.

The contributions to the systematic error include the uncertainties due to the tracking efficiency (2% per

track), particle identification efficiency (4-14%, depending on the mode) and the modeling of the likelihood ratio requirement (2%). The error in kaon identification efficiency is obtained from kinematically selected $D^{*+} \to D^0\pi^+$, $D^0 \to K^-\pi^+$ in the data while the error in proton/antiproton identification is determined using $\Lambda/\bar{\Lambda}$ samples. The systematic error due to the modeling of the likelihood ratio cut is determined using $B^+ \to \bar{D}^0\pi^+$ events reconstructed in data. The systematic error in the yields of the $M_{\rm bc}$ fit were determined by varying the mean and $\sigma$ of the signal and the shape parameters of the background. To account for the possibility of background from non-resonant modes that may contribute to the $M_{\rm bc}$ distribution, we include the yields observed in the $\eta_c$ mass sideband (8-14% of the signal depending on the mode) as an asymmetric systematic error. The sources of systematic error are combined in quadrature to obtain the total systematic error, which is given in Table II.

TABLE I. Signal yields from $M_{\rm bc}$ and $\Delta E$ fits, statistical significances and MC reconstruction efficiencies. Errors are statistical only.

| $B^+ \to \eta_c K^+$ | $\Delta E$ Yield | $M_{\rm bc}$ Yield | Signif.($M_{\rm bc}$) | $\epsilon(\%)$ |
|---|---|---|---|---|
| $\eta_c \to K_S^0 K^-\pi^+$ | $74.8 \pm 10.4$ | $81.6 \pm 10.3$ | $12.2\sigma$ | 16.4 |
| $\eta_c \to K^+ K^-\pi^0$ | $26.5 \pm 7.8$ | $31.8 \pm 7.0$ | $6.3\sigma$ | 8.8 |
| $\eta_c \to p\bar{p}$ | $16.3 \pm 4.2$ | $17.7 \pm 4.4$ | $7.5\sigma$ | 34.0 |
| $\eta_c \to K^{*0} K^-\pi^+$ | $22.0 \pm 5.8$ | $20.8 \pm 5.4$ | $5.8\sigma$ | 5.1 |

| $B^0 \to \eta_c K_S^0$ | $\Delta E$ Yield | $M_{\rm bc}$ Yield | Signif.($M_{\rm bc}$) | $\epsilon(\%)$ |
|---|---|---|---|---|
| $\eta_c \to K_S^0 K^-\pi^+$ | $19.6 \pm 5.4$ | $23.0 \pm 5.4$ | $6.8\sigma$ | 15.5 |
| $\eta_c \to K^+ K^-\pi^0$ | $19.9 \pm 5.7$ | $17.1 \pm 5.1$ | $4.7\sigma$ | 9.5 |
| $\eta_c \to p\bar{p}$ | $7.0 \pm 3.0$ | $6.8 \pm 2.6$ | $5.0\sigma$ | 34.9 |
| $\eta_c \to K^{*0} K^-\pi^+$ | $0.2 \pm 1.7$ | $2.2 \pm 1.8$ | $1.6\sigma$ | 3.75 |

TABLE II. Product branching fractions for $B \to \eta_c K$ decay modes ($10^{-6}$).

| | |
|---|---|
| $\mathcal{B}(B^+ \to \eta_c K^+) \times \mathcal{B}(\eta_c \to K_S^0 K^-\pi^+)$ | $(23.2 \pm 2.9^{+2.8}_{-3.8})$ |
| $\mathcal{B}(B^+ \to \eta_c K^+) \times \mathcal{B}(\eta_c \to K^+ K^-\pi^0)$ | $(11.4 \pm 2.5^{+1.1}_{-1.8})$ |
| $\mathcal{B}(B^+ \to \eta_c K^+) \times \mathcal{B}(\eta_c \to p\bar{p})$ | $(1.64 \pm 0.41^{+0.17}_{-0.24})$ |
| $\mathcal{B}(B^+ \to \eta_c K^+) \times \mathcal{B}(\eta_c \to K^{*0} K^-\pi^+)$ | $(19.3 \pm 5.0^{+3.4}_{-3.8})$ |
| | |
| $\mathcal{B}(B^0 \to \eta_c K^0) \times \mathcal{B}(\eta_c \to K_S^0 K^-\pi^+)$ | $(20.1 \pm 4.7^{+3.0}_{-4.5})$ |
| $\mathcal{B}(B^0 \to \eta_c K^0) \times \mathcal{B}(\eta_c \to K^+ K^-\pi^0)$ | $(16.6 \pm 5.0^{+1.8}_{-1.8})$ |
| $\mathcal{B}(B^0 \to \eta_c K^0) \times \mathcal{B}(\eta_c \to p\bar{p})$ | $(1.79 \pm 0.68^{+0.19}_{-0.25})$ |
| $\mathcal{B}(B^0 \to \eta_c K^0) \times \mathcal{B}(\eta_c \to K^{*0} K^-\pi^+)$ | $(8.1 \pm 6.6 \pm 1.4)$ |
| | $< 29$ at 90% C.L. |

The product branching fractions are given in Table II for all modes in which signals are observed. Since many of the $\eta_c$ branching fractions are poorly determined

and in some cases there are conflicting measurements, we quote $B$ branching fractions for the $\eta_c \to K_S^0 K^-\pi^+$ and $\eta_c \to K^-K^+\pi^0$ modes only. The $\eta_c \to K_S^0 K^-\pi^+$ mode is the most precisely and reliably measured mode and the branching fraction for the $\eta_c \to K^-K^+\pi^0$ mode is related by isospin. We use $\mathcal{B}(\eta_c \to K_S^0 K^-\pi^+) = 1/3 \times (0.055 \pm 0.017)$ where $1/3$ is the product of the appropriate Clebsch-Gordon coefficient and intermediate $K^0$ branching fraction. We assume that the experimental systematic errors in the $\eta_c \to K_S^0 K^-\pi^+$ and $\eta_c \to K^-K^+\pi^0$ modes are uncorrelated. We assume equal production of $B^+B^-$ and $B^0\bar{B}^0$ pairs and do not include an additional systematic error for the uncertainty in this assumption. We find

$$\mathcal{B}(B^+ \to \eta_c K^+) = (1.25 \pm 0.14^{+0.10}_{-0.12} \pm 0.38) \times 10^{-3}$$

and

$$\mathcal{B}(B^0 \to \eta_c K^0) = (1.23 \pm 0.23^{+0.12}_{-0.16} \pm 0.38) \times 10^{-3}.$$

The first error is statistical, the second error is systematic and the third error is due to the uncertainty in the $\eta_c$ branching fraction scale. When the $\eta_c$ branching fractions for the other modes are better determined, absolute $B$ branching fractions for these modes can be extracted from our results.

In the $B^0 \to \eta_c K^{*0}$, $K^{*0} \to K^+\pi^-$ channel, the $\eta_c$ is reconstructed in the $K_S^0 K^\pm\pi^\mp$ mode. Since this mode is a pseudoscalar to pseudoscalar-vector decay, by angular momentum conservation, the cosine of the $K^*$ helicity angle $(\cos\theta_H)$ follows a $\cos^2\theta_H$ distribution; we select events with $|\cos\theta_H| > 0.4$. We also investigate $B\bar{B}$ background and find that this background can be removed by applying vetos to events with combinations that are consistent with $J/\psi \to K_S^0 K\pi$, $J/\psi \to K^+K^-\pi^+\pi^-$, $\psi(2S) \to K_S^0 K\pi$, $\eta_c(2S) \to K_S^0 K\pi$, $\chi_{c1} \to K_S^0 K\pi$, $\eta_c \to K^+K^-\pi^+\pi^-$, $D_s^+ \to K_S^0 K^+$ and $D_s \to K^-K^+\pi$. The detection efficiency for these selection requirements is $(7.95 \pm 0.12)\%$.

After applying these requirements, a fit to the $M_{\rm bc}$ distribution yields a signal of $33.7 \pm 6.7$ events for $B^0 \to \eta_c K^{*0}$ with a statistical significance of $7.7\sigma$. [11] The $M_{\rm bc}$ distribution is shown in Fig. 3(a). The yields from the $\Delta E$ fit, shown in Fig. 3(b) ($30\pm7$ events), the $\eta_c$ invariant mass distribution ($24\pm7$ events) and the $K^+\pi^-$ invariant mass distribution ($27 \pm 8$ events) are consistent with the yield from the $M_{\rm bc}$ fit.

To evaluate the contribution from non-resonant $B^0 \to K_S^0 K^+\pi^- K^*$ as well as the remaining $B\bar{B}$ backgrounds that peak in the $M_{\rm bc}$ distribution, we select events in the $\eta_c$ sideband [15] and repeat the $M_{\rm bc}$ fit. We find no significant signal. By using the ratio of the yields in the $\eta_c$ signal and sideband regions determined from MC, we estimate the contributions of such backgrounds to be $3.9\pm4.2$ events, consistent with zero. We use the $K^*$ sideband [15] to estimate the non-resonant $B^0 \to \eta_c K\pi$ decay

component and obtain $-0.6 \pm 3.3$ events. These possible background contributions are not subtracted in the branching fraction measurement, but instead are treated as systematic uncertainties. We find

$$\mathcal{B}(B^0 \to \eta_c K^{*0}) = (1.62 \pm 0.32^{+0.24}_{-0.34} \pm 0.50) \times 10^{-3}.$$

To take into account the possibility of $B\bar{B}$ background, we conservatively include asymmetric systematic errors from the results of the fits to the $\eta_c(-12\%)$ and $K^*$ $(-8\%)$ sidebands. Other sources of systematic error are the uncertainties in the track reconstruction efficiency ($\pm 2\%$ per track), the parameters in the $M_{\rm bc}$ fit ($\pm 7\%$), particle identification ($\pm 6\%$) and the number of $B^0 \bar{B}^0$ events.

From the results for the branching fractions for $B^0 \to \eta_c K^0$ and $B^0 \to \eta_c K^{*0}$ determined above, we can determine the ratio $R_{\eta_c} = \mathcal{B}(B^0 \to \eta_c K^{*0})/\mathcal{B}(B^0 \to \eta_c K^0)$. The uncertainty from the $\eta_c$ branching fraction scale cancels in the ratio. We find

$$R_{\eta_c} = 1.33 \pm 0.36^{+0.24}_{-0.33}.$$

Our result can be compared to calculations of this ratio in models based on factorization and is consistent with the range 1.02-2.57 predicted by Gourdin, Keum and Pham. [16].
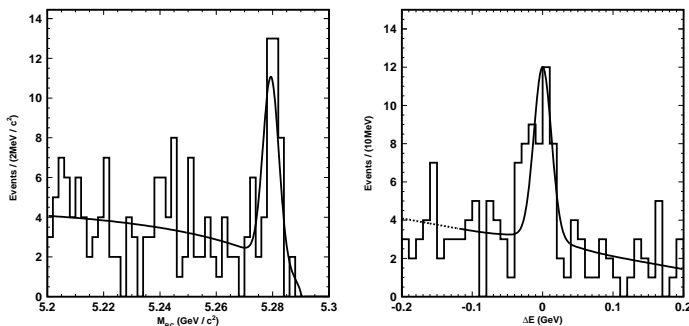


FIG. 3. (a) $M_{\rm bc}$ and (b) $\Delta E$ distributions for $B \to \eta_c K^{*0}$ candidates.

The branching fractions reported in this paper for $B^+ \to \eta_c K^+$ and $B^0 \to \eta_c K^0$ using $\eta_c \to K\bar{K}\pi$ decays are more precise than previous results [17]. The result for the $B^+ \to \eta_c K^+$ branching fraction is somewhat higher than the CLEO measurement, while the $B^0 \to \eta_c K^0$ result is consistent. Several additional $\eta_c$ modes including $\eta_c \to p\bar{p}$, $\eta_c \to K^- K^+ \pi^0$ and $\eta_c \to K^{*0} K^- \pi^+$ have been used and increase the fraction of $\eta_c$ decays that can be reconstructed for $CP$ violation measurements. With the large samples of $B \to \eta_c K$ decays now available, we are able to determine the mass and width of the $\eta_c$ meson. We find $M(\eta_c) = 2979.6 \pm 2.3 \pm 1.6$ MeV and $\Gamma(\eta_c) = 29 \pm 8 \pm 6$ MeV. In addition, we report the first observation of the $B^0 \to \eta_c K^{*0}$ decay, which is an $CP$ eigenstate when $K^{*0} \to K^0_S \pi^0$.

[1] K. Abe *et al.* (Belle Collaboration), Phys. Rev. Lett. **87**, 091802 (2001).

[2] K. Abe *et al.* (Belle Collaboration), Phys. Rev. D **66**, 071102(R) (2002).

[3] B. Aubert *et al.* (BaBar Collaboration), hep-ex/0207042, to appear in Phys. Rev. Lett.

[4] N.G. Deshpande and J. Trampetic, Phys. Lett. B **339**, 270 (1994).

[5] The inclusion of the charge conjugate mode is implied.

[6] KEKB B Factory Design Report, KEK Report 95-1, 1995, unpublished.

[7] A. Abashian *et al.* (Belle Collaboration.), Nucl. Instr. and Meth. A **479**, 117 (2002).

[8] The vertex $\chi^2$ requirement is $< 50$ for all modes except for $\eta_c \to K^0_S K^- \pi^+$, where a less restrictive cut $< 100$ is used.

[9] The Fox-Wolfram moments were introduced in G.C. Fox and S. Wolfram, Phys. Rev. Lett. **41**, 1581 (1978). The Fisher discriminant used by Belle is described in K. Abe *et al.*, Phys. Rev. Lett. **87**, 101801 (2001) and K. Abe *et al.*, Phys. Lett. B **511**, 151 (2001).

[10] H. Albrecht *et al.* (ARGUS Collaboration), Phys. Lett. B 241, 278 (1991).

[11] The significances are calculated from the change in the likelihood when the signal yield is set to zero.

[12] G.J. Feldman and R.D. Cousins, Phys. Rev. D **57**, 3873 (1998).

[13] Using an implementation of the Cousins-Highland method described in J. Conrad et al., hep-ex/020213 (submitted to PRD) and J. Conrad et al., hep-ex/0206034 to incorporate systematic uncertainties in the upper limit, we obtain a slightly more restrictive limit of 7.1 events on the yield. This corresponds to an upper limit of $26 \times 10^{-6}$ rather than the value $29 \times 10^{-6}$ given in the text.

[14] D.E. Groom *et al.* (Particle Data Group), Eur. Phys. J. C **15**, 1 (2000).

[15] The mass regions $2.74 < M_{K_S K^\pm \pi^\mp} < 2.84$ GeV/c$^2$ and $3.25 < M_{K_S K^\pm \pi^\mp} < 3.35$ GeV/$c^2$ are used as the $\eta_c$ sideband. The range $1.60 < M_{K^- \pi^+} < 1.79$ GeV/c$^2$ is used as the $K^*$ sideband.

[16] M. Gourdin, Y. Y. Keum and X.Y. Pham, Phys. Rev. D **52**, 1597 (1996).

[17] K. Edwards *et al.* (CLEO Collaboration), Phys. Rev. Lett. **86**, 30 (2001).